Towards predicting the stability of protein-stabilized emulsions

Delahaije, R. J. B. M., Gruppen, H., Giuseppin, M. L. F., & Wierenga, P. A.

Towards predicting the stability of protein-stabilized emulsions

Roy J.B.M. Delahaije,[1] Harry Gruppen,[1] Marco L.F. Giuseppin,[2] and Peter A. Wierenga[1,*]

[1]Laboratory of Food Chemistry, Wageningen University, Bornse Weilanden 9, 6708 WG, Wageningen, The Netherlands.

[2]AVEBE, Prins Hendrikplein 20, 9641 GK, Veendam, The Netherlands.

ABSTRACT

The protein concentration is known to determine the stability against coalescence during formation of emulsions. Recently, it was observed that the protein concentration also influences the stability of formed emulsions against flocculation as a result of changes in the ionic strength. In both cases, the stability was postulated to be the result of a complete (i.e. saturated) coverage of the interface. By combining the current views on emulsion stability against coalescence and flocculation with new experimental data, an empiric model is established to predict emulsion stability based on protein molecular properties such as exposed hydrophobicity and charge. It was shown that besides protein concentration, the adsorbed layer (i.e. maximum adsorbed amount and interfacial area) dominates emulsion stability against coalescence and flocculation. Surprisingly, the emulsion stability was also affected by the adsorption rate. From these observations, it was concluded that a completely covered interface indeed ensures the stability of an emulsion against coalescence and flocculation. The contribution of adsorption rate and

adsorbed amount on the stability of emulsions was combined in a surface coverage model. For this model, the adsorbed amount was predicted from the protein radius, surface charge and ionic strength. Moreover, the adsorption rate, which depends on the protein charge and exposed hydrophobicity, was approximated by the relative exposed hydrophobicity (Q_H). The model in the current state already showed good correspondence with the experimental data, and was furthermore shown to be applicable to describe data obtained from literature.

KEYWORDS

Coalescence, flocculation, model, adsorption rate, adsorbed amount, surface coverage

CONTENTS

1. INTRODUCTION

Proteins are widely used for the stabilization of emulsions [1-3]. The four main destabilization mechanisms affecting a protein-stabilized emulsion are creaming, coalescence, flocculation and Ostwald ripening [4]. During emulsion formation, proteins are typically considered to adsorb to the interface, and thereby stabilize the emulsion against coalescence [5]. After formation, the emulsion stability against flocculation is described to be determined by the charge of the adsorbed protein layer [4, 6]. For oil-in-water emulsions destabilization by Ostwald ripening is

often neglected, since typical triglyceride oils used in food emulsions, such as corn and peanut oil, have a low solubility in water [8-10] and can therefore not diffuse through the water phase.

Next, the link between coalescence and flocculation of emulsions and the protein molecular properties are reviewed. Based on this information and recent work, an empiric model is proposed that links the stability against coalescence and flocculation to the protein molecular properties such as size, charge and hydrophobicity.

1.1. Stability against coalescence

Coalescence is reported to be the main destabilization mechanism during emulsion formation [5]. During formation, droplets with a certain defined size ($d_{3,2,\ min}$) will be formed, depending on for instance power input, interfacial tension and mass density of the continuous phase [7]. If sufficient protein is present to cover the newly formed interface (i.e. emulsion droplet) completely, the droplets are considered to be stable ($d_{3,2} = d_{3,2,\ min}$) (figure 1A). A lack of protein in the continuous phase will lead to incomplete coverage of the interface. This in turn results in coalescence during formation, until an interfacial area (i.e. droplet size) is reached for which there is sufficient protein present (figure 1A). Coalescence can therefore be prevented by increasing the protein concentration in the continuous phase. This explains the two characteristic concentration regimes which are observed during emulsion formation (i.e. protein-poor and protein-rich regime) [2, 11].

In the protein-poor regime (regime I), the droplet size ($d_{3,2}$) is equal to the minimal droplet size for which the complete interface can be (sufficiently) covered with protein, as described in equation 1 [11]. The maximum adsorbed amount (Γ_{max}) in this regime corresponds closely to that of a monolayer [2, 12, 13]. Consequently, if the droplet size, calculated from equation 1 [11], is

plotted against protein concentration, different curves are obtained depending on volume fraction oil (Φ_{oil}) and Γ_{max} (figure 2A). Recently, the maximum adsorbed amount for a protein has recently been described to be influenced by its molecular properties (i.e. size and charge) and system conditions (i.e. ionic strength) [14], as was previously shown for hard-sphere colloids [15-17].

In the protein-rich regime (regime II), the droplet size is only affected by factors such as power input, interfacial tension and mass density of the continuous phase ($d_{3,2} = d_{3,2,\,min}$) (equation 2).

$$d_{3,2(I)} \approx \frac{6\Phi_{oil}\Gamma_{max}}{(1-\Phi_{oil})C} \qquad (1)$$

$$d_{3,2(II)} = d_{3,2,min} \qquad (2)$$

where Φ_{oil} is the volume fraction oil [-], Γ_{max} is the maximum adsorbed amount [mg m^{-2}] and C is the protein concentration [g L^{-1}].

Assuming the validity of equations 1 and 2, all curves are expected to superimpose onto a single curve by correcting for the C, Φ_{oil} and Γ_{max} (figure 2B). In this curve one critical point (F_s) is identified, where all curves shift from the protein-poor to the protein-rich regime. Using this stability factor (i.e. F_s), the critical protein concentration (C_{cr}) for any Φ_{oil} and Γ_{max} can be calculated by replacing the $d_{3,2}$ with the $d_{3,2,\,min}$ of the system. In addition to these parameters (i.e. C, Φ_{oil} and Γ_{max}), the shift between the protein-poor and protein-rich regime, and thereby C_{cr}, has recently been reported to depend on the exposed hydrophobicity (Q_H) [18]. This was postulated to be caused by the fact that an increase of Q_H decreases the barrier for adsorption to the air-water interface, resulting in a higher adsorption rate [14, 19]. The maximum adsorbed amount at the air-water and the oil-water interface has, on the other hand, been described to be independent of the exposed hydrophobicity of the protein [14, 19, 20]. A higher adsorption rate therefore translates into faster coverage of the interface. This helps to prevent coalescence during

formation, and is consequently expected to result in the formation of smaller droplets under similar conditions. Accordingly, the adsorption rate has recently been proposed to affect the initial droplet size of emulsions stabilized by surfactants and proteins [21]. In summary, the critical concentration is expected to decrease with increasing exposed hydrophobicity due to an increase of the adsorption rate (k_{adsorb}). Therefore, it is proposed that equation 1 for the protein-poor regime can be approximated by equation 3.

$$d_{3,2(I)} \approx \frac{6\Phi_{oil}\Gamma_{\max}}{(1-\Phi_{oil})Ck_{adsorb}} \qquad (3)$$

The importance of adsorption rate, even under turbulent flow, is demonstrated by the fact that Gum Arabic, which is described to adsorb slower to the oil-water interface than β-lactoglobulin [22], was described to form larger emulsions droplets than WPI at an equal concentration [23, 24].

1.2. Stability against flocculation

Flocculation is reported to be the main destabilization mechanism during emulsion stabilization [6, 20]. The occurrence of flocculation has often been explained based on the interactions (e.g. electrostatic repulsion) between emulsion droplets [4, 6, 25]. In case of net repulsive interactions (i.e. at a pH away from the iso-electric point (pI) and at low ionic strength), the electrostatic repulsion between the adsorbed layer as a result of protein charge prevents flocculation. If the charge decreases (i.e. shift of pH towards pI and/or an increase of the ionic strength), the electrostatic repulsion decreases and the emulsion droplets may flocculate. However, recent experiments have indicated that not only the inter-droplet interactions, but also the adsorbed amount changes with conditions (i.e. ionic strength) [14, 26]. A change in adsorbed amount latter was also observed for particle [15-17] and protein adsorption [27-29] at solid-liquid interfaces.

The maximum adsorbed amount (Γ_{max}) was shown to increase with increasing ionic strength due to a decrease of the effective radius of the protein (as a result of a decrease of the Debye screening length) [17, 30-33]. Therefore, more protein is needed to reach the maximum adsorbed amount and completely cover the interface. At higher protein concentrations, more protein is present to supplement a partially covered interface, thereby resulting in an increased stability against flocculation [18, 20] (figure 1B). This shows that both the stability during formation (figure 1A) and after changes in the conditions (figure 1B) increases with increasing protein concentration. It is, therefore, postulated that equation 3, which accounts for the adsorbed amount (Γ_{max}) at the interface, describes the stability during formation, as well as the stability after changes in conditions.

1.3. Theoretical prediction of the maximum adsorbed amount

The maximum adsorbed amount was shown to be an important factor affecting the emulsion stability against coalescence and flocculation. Therefore, it is of interest to quantitatively predict the adsorbed amount for different proteins under different conditions. Recently, the Random Sequential Adsorption (RSA) model with the effective hard-particle concept [34-36] was successfully applied to describe Γ_{max} for globular proteins at the air-water interface [14]. The theoretical maximum adsorbed amount for a close-packed monolayer ($\Gamma_{mono,\ theory}$) was predicted using equation 4 [14]. In accordance with the RSA model, this prediction describes globular proteins as hard disks adsorbing at a two-dimensional interface. At the jamming limit, the saturation coverage (θ_∞) is approximated to be 0.547 [30, 37-39].

$$\Gamma_{mono,theory} = \frac{10^3 M_w}{\pi R_{eff}{}^2 N_a} \theta_\infty \qquad (4)$$

156 in which $\Gamma_{mono,\ theory}$ is the theoretical maximum adsorbed amount of a close-packed
157 monolayer [mg m^{-2}], M_w is the molecular mass of the protein [g mol^{-1}], R_{eff} is the
158 effective hard-sphere radius of an adsorbed protein [m], N_a is the Avogadro constant
159 [6.022 x 10^{23} mol^{-1}] and θ_∞ is the saturation coverage, which has a value of 0.547 for
160 irreversible bound, non-diffusing particles [30, 37-39].
161 The RSA model was originally developed for the adsorption of hard sphere, non-
162 interacting particles [40]. Later, the effective hard-sphere particle concept was introduced
163 to account for interacting particles [34-36]. The validity of the latter concept to describe
164 Γ_{max} of globular proteins indicates that adsorbed globular proteins can be depicted as hard
165 sphere particles with a soft shell as a result of their charge. The effective radius of a
166 charged particle (i.e. globular protein) adsorbed at an interface can be estimated by the
167 hard-sphere approximation as the sum of the protein radius (R_p) and a characteristic
168 distance due to electrostatic repulsion [17, 30-33] (equation 5) [14]. Assuming a constant
169 surface charge, the effective radius (R_{eff}) can be described by equation 6 [14].

$$R_{eff} = R_p - \tfrac{1}{2}\ln\left(\frac{U_{driving}}{2\pi\varepsilon_0\varepsilon_r R_p \Psi_0{}^2}\right)\kappa^{-1} \qquad (5)$$

$$R_{eff} = R_p - \tfrac{1}{2}\ln\left(\frac{x}{R_p}\right)\kappa^{-1} \qquad (6)$$

170 where R_p is the protein radius [m], $U_{driving}$ is the adsorption driving interaction [J], ε_0 is
171 the dielectric constant of a vacuum [8.85 x 10^{-12} C^2 J^{-1} m^{-1}], ε_r is the relative dielectric
172 constant of the medium [80], Ψ_0 is the surface potential [V], κ^{-1} is the Debye screening
173 length [m] and x is a constant [m]. The constant was found to be 1.77 x 10^{-9} m for

β-lactoglobulin and ovalbumin and 0 m for lysozyme at pH 7.0 [14]. The radius of a globular protein and the Debye screening length can be calculated using equations 7 [41] and 8 [42], respectively.

$$R_p = \left(\frac{3\nu M_w}{4\pi N_a} \right)^{\frac{1}{3}} \quad (7)$$

$$\kappa^{-1} = \sqrt{\frac{2N_a e^2 I}{\varepsilon_0 \varepsilon_r k_B T}} \quad (8)$$

in which v is the partial specific volume [0.73 x 10^{-6} m^3 g^{-1}] [41], e is the elementary charge [1.602 x 10^{-19} C], I is the ionic strength [mol m^{-3}], k_B is the Boltzmann constant [1.38 x 10^{-23} J K^{-1}] and T is the temperature [K].

It is important to realize that the RSA model assumes that: 1) particles adsorb randomly on the interface, depending on the fact whether or not they encounter an empty spot. 2) adsorbed particles do not desorb from the interface; 3) adsorbed particles do not diffuse on the interface [43]. For globular proteins, the first two assumptions have been validated [44], whereas the latter can be debated. Two limitations of the RSA model are that it does not account for multilayer adsorption and unfolding at the interface. The validity of the model for globular proteins means that, under the tested conditions, the structural changes upon adsorption are not significant and that the proteins do not form multilayers. This is in contrast with commonly held views that proteins unfold at interfaces [45, 46] and may form multilayers [5]. Several studies, however, suggested that protein unfolding at the interface is concentration dependent [47, 48]. At low protein concentrations, the timescale of adsorption is slower than the timescale of unfolding and spreading. At higher protein concentrations, the opposite is the case (i.e. the timescale of adsorption is faster than the timescale of unfolding and spreading), thereby preventing unfolding and spreading. For

β-lactoglobulin at the air-water interface, no effect of protein concentration on the adsorbed amount was observed at concentrations exceeding 0.1 g L^{-1} [49], showing that unfolding becomes negligible above this concentration. At the same time, to form an emulsion or foam, a certain minimal amount of protein needs to adsorb within the timescale of formation. Consequently, in each case where adsorption is sufficiently fast, the protein concentration will be so high that it is even in the consensus view unlikely for proteins to significantly unfold.

1.4. Towards an empiric model for emulsion stability

The previous, especially equation 3, indicates that it should be possible to describe and to predict emulsion stability based the adsorption rate and the adsorbed amount. Therefore, the aim of this study is to confirm this view with new experimental data, and to establish a first empiric model. To accomplish this, the effect and contribution of C, Γ_{max} and k_{adsorb} on emulsion stability was studied for different proteins at various ionic strengths.

2. MATERIALS AND METHODS

2.1. Materials

Lysozyme (Lys; L6876, Lot nº 051K7028; purity > 90 % based on size-exclusion chromatography), β-lactoglobulin (β-lg; L0130, Lot nº SLBC2933V; protein content of 99 % (N x 6.38), of which 94 % β-lactoglobulin based on SDS-PAGE) and ovalbumin (Ova; A5503 Lot nº 031M7008V; protein content of 98 % (N x 6.22), of which 92 % ovalbumin based on agarose gel electrophorese) were purchased from Sigma-Aldrich (St.

Louis, MO, USA). All other chemicals were of analytical grade and purchased from either Sigma-Aldrich or Merck (Darmstadt, Germany).

2.2. Quantification of exposed hydrophobicity

The increase in fluorescence intensity upon binding of 8-anilino-1-napthalenesulfonic acid (ANSA) to the accessible hydrophobic regions of the protein is used as a measure of the protein surface hydrophobicity [50]. The proteins were dissolved in 10 mM sodium phosphate buffer pH 7.0 in a concentration of 0.1 g L^{-1}. The measurements were performed on a Varian Cary Eclipse fluorescence spectrophotometer (Agilent Technologies, Santa Clara, CA, USA) as described elsewhere [14].

2.3. Zeta potential of protein solutions

Zeta potentials of the proteins in solution were determined with a Zetasizer Nano ZSP (Malvern Instruments, Worcestershire, UK) using the laser Doppler velocimetry technique. The proteins (10 g L^{-1}) were dissolved in 10 mM sodium phosphate buffer pH 7.0. The measurements were performed at 25 °C and 40 Volt. The results of five sequential runs were averaged. Zeta potentials were calculated with Henry's equation [51] (equation 9).

$$\zeta = \frac{3\eta\mu_e}{2\varepsilon F(\kappa\alpha)} \qquad (9)$$

in which ζ is the zeta potential [V], η is the viscosity [0.8872 x 10^{-3} Pa s], μ_e is the electrophoretic mobility [m^2 V^{-1} s^{-1}], ε is the dielectric constant of the medium [7.08 x 10^{-10} C^2 J^{-1} m^{-1}] and $F(\kappa\alpha)$ is Henry's function [-], which equals 1.5 using the Smoluchowski approximation [51].

2.4. Emulsification

The protein solutions were mixed with 10 %(v/v) sunflower oil. A pre-emulsion was prepared using an Ultra turrax Type T-25B (IKA, Staufen, Germany) at 9500 rpm for 1 min. Subsequently, the pre-emulsion was passed 30 times through a Labhoscope 2.0 laboratory scale high-pressure homogenizer (Delta Instruments, Drachten, The Netherlands) operated at 15 MPa. The solutions were cooled on ice-water during homogenization. Three different sets of experiments were performed:

2.4.1. Effect of protein concentration

β-Lactoglobulin was dissolved in 10 mM sodium phosphate buffer pH 7.0 at concentrations of 1, 2, 2.5, 3, 4, 5, 7.5 and 10 g L^{-1}.

2.4.2. Effect of ionic strength

β-Lactoglobulin was dissolved in 10 mM sodium phosphate buffer pH 7.0 in the absence or presence of 20 and 190 mM NaCl at concentrations of 1, 2, 2.5, 3, 4, 5, 7.5 and 10 g L^{-1}. Moreover, the ionic strength of the β-lactoglobulin emulsions prepared in the absence of NaCl was adjusted to 30 and 200 mM with 2 M NaCl after emulsification.

2.4.3. Effect of adsorption rate (k_{adsorb})

β-Lactoglobulin, ovalbumin and lysozyme were dissolved in 10 mM sodium phosphate buffer pH 7.0 at concentrations of 1, 2, 2.5, 3, 4, 5, 7.5 and 10 g L^{-1}, 1, 2.5, 5, 7.5, 10, 15 and 20 g L^{-1} and 2.5, 5, 10, 15, 20, 25 g L^{-1}, respectively.

Subsequently, the emulsions were stored for 24 hours at 20 °C prior to further analysis. For selected samples, it was confirmed that no significant changes occurred during this storage period.

2.5. Zeta potential of emulsion droplets

Zeta potentials of the emulsion droplets were determined with a Zetasizer Nano ZS (Malvern Instruments) using the laser Doppler velocimetry technique. The emulsions were diluted 500 times to prevent multiple scattering. The measurements were performed at 25 °C and 40 Volt. The results of five sequential runs were averaged. Zeta potentials were calculated with Henry's equation [51] (equation 9).

2.6. Determination of droplet size

2.6.1. Diffusing wave spectroscopy (DWS)

As indication of the droplet size *in situ*, without dilution, DWS measurements were performed as described previously [52]. The autocorrelation function was averaged from five sequential runs of 120 seconds. Subsequently, the autocorrelation functions were normalized by dividing the obtained $g_2(t)$-1 values by the maximum measured value. Normalized autocorrelation functions were then fitted using equation 11. This was derived from Ruis et al. [52], assuming that $<\Delta r^2(t)> = 6Dt^p$ for $p < 1 = \alpha t^x$ for $x < 1$.

$$g_2(t) - 1 \approx (e^{-<\Delta r^2(t)>})^2 \approx e^{-\alpha t^x} \qquad (11)$$

The decay time ($\tau_{1/2}$), which is defined as the time at which $g_2(t)$-1 decayed to half of its initial value, was determined using the fitted equation. An increase of the decay time is related to decreased droplet mobility [53, 54]. Although DWS in the tested regime (droplet size and Φ) has been described to be suitable for sizing [55], the droplet mobility is only used as an indication of the droplet size.

283 2.6.2. Laser diffraction

284 The average droplet size of the emulsions was measured using laser light diffraction
285 (Mastersizer 2000, Malvern Instruments) equipped with a Hydro SM sample dispersion
286 unit. The droplet size was calculated using the general purpose model with a refractive
287 index of 1.45 and 1.33 for the droplet and continuous phase, respectively. The volume-
288 surface average diameter ($d_{3,2}$) (equation 10) was reported as an average of at least five
289 runs.

$$d_{3,2} = \sum N_i d_i^{\,3} / \sum N_i d_i^{\,2} \qquad (10)$$

290 in which N_i and d_i represent the number and diameter of droplets of size class i, respectively.

291

292 **3. RESULTS AND DISCUSSION**

293 *3.1. Colloidal model*

294 Based on a simplified colloidal model (i.e. DLVO interactions), it is expected that
295 flocculation of emulsion droplets with a similar radius would occur when the zeta
296 potential of the emulsion droplets decreases below a certain critical value (i.e. decrease of
297 the electrostatic repulsion) [42]. As expected, an increase of the ionic strength (i.e.
298 decrease of zeta potential) destabilizes the emulsion with a low protein concentration (in
299 this case 2 g L^{-1}). This resulted in flocculation as indicated by a longer decay time ($\tau_{1/2}$),
300 as measured by DWS (figure 3).

301 An increase of the ionic strength leads to a similar decrease of the zeta potential of the
302 emulsion with a higher protein concentration (in this case 5 g L^{-1}). Surprisingly, the
303 decrease does not lead to salt-induced flocculation for this emulsion. This observation is
304 explained by the fact that at an increased ionic strength more protein is needed to

completely cover the interface. The emulsion with a low protein concentration cannot comply with the need for protein (i.e. protein-poor regime). As a result, the interface cannot be completely covered, leading to flocculation of emulsion droplets. If sufficient protein is present in the continuous phase (i.e. at 5 g L^{-1}; protein-rich regime), the excess protein adsorbs to the bare interface and stabilizes the emulsion against flocculation. This proposed view is referred to as the surface coverage model.

To confirm that this stabilizing effect results from an increase of the protein concentration, the protein concentration of the emulsion prepared at 2 g L^{-1} is supplemented to a final concentration of 5 g L^{-1}. As expected, this also results in an emulsion which is stable against salt-induced flocculation. It is therefore concluded that adsorbed layer, as considered in the surface coverage model, is of importance for the stability of the emulsions. This is in line with previous studies showing the importance of excess protein in the continuous phase for the stability against salt-induced flocculation [18, 20].

A similar behaviour was observed for emulsions prepared in the presence of NaCl and for emulsions of which the ionic strength was adjusted after emulsification. This shows the analogy between emulsion formation and stabilization. Moreover, it confirms that, as described in the surface coverage model, the protein concentration relative to the adsorbed amount and interfacial area is important for both processes (as described by equations 1 and 3).

3.2. Surface coverage model

Based on the above, the stability of a protein-stabilized emulsion during formation and after changes in system conditions can be considered to be determined by the fact whether the protein covers the interface completely. Since interfacial coverage is thought to be the dominant factor, it will be referred to as the surface coverage model. However, so far the model only comprises of a view, validated by some qualitative experimental results. In a first approach, the effect of molecular properties and system conditions on emulsion stability during formation (i.e. stability against coalescence) was studied to come to an empiric model.

3.2.1. Effect of adsorption rate (k_{adsorb})

To determine the effect of the adsorption rate (at a constant ionic strength of 10 mM), the decay time and average droplet size of emulsions stabilized by three different proteins (lysozyme, ovalbumin and β-lactoglobulin) was determined. This shows that the critical protein concentration (C_{cr}), which marks the transition from the protein-poor to the protein-rich regime, shifts from ≥ 25 g L^{-1} for lysozyme to ~ 10 g L^{-1} for ovalbumin and 2 g L^{-1} for β-lactoglobulin (figure 4A). This difference is also reflected in the average droplet size ($d_{3,2}$) at 5 g L^{-1} which varies from 7.33 μm for lysozyme to 0.50 and 0.26 μm for ovalbumin and β-lactoglobulin, respectively (figure 4B). Based on equation 1, the difference between the proteins can be explained by a shift of the maximum adsorbed amount (Γ_{max}). To test this, curves were plotted as described by equation 1, using Γ_{max} calculated assuming a full monolayer coverage ($\Gamma_{mono,\ theory}$) predicted by a model described previously [14] (table 1). After this correction, the curves of the different proteins do still not superimpose (figure 4C). This shows that the observed differences

between the proteins cannot only be explained by differences in adsorbed amount. Therefore, the initial adsorption rate (k_{adsorb}) is included as described in equation 3. At a given concentration and ionic strength, the adsorption rate was described to increase with increasing relative exposed hydrophobicity [14, 49]. Therefore, the relative exposed hydrophobicity of the protein (Q_H) was used as an indication for k_{adsorb} (table 1).

When corrected for Q_H, all curves superimpose (figure 4D). All emulsions above the stability factor (F_s) of 2 are in the protein-rich regime. This confirms that the critical protein concentration is also affected by the initial adsorption rate (i.e. affinity of the protein towards adsorption to the interface).

3.2.2. Effect of adsorbed amount (Γ_{max})

To determine the effect of the adsorbed amount, the droplet size of emulsions stabilized by β-lactoglobulin at different ionic strengths (i.e. 10 and 200 mM) were determined. An increase of the ionic strength resulted in an increase of the average droplet size and decay time measured by static light scattering (SLS) and DWS, respectively (figures 5A and B). The increase of the droplet size is also reflected in a shift of the transition between the protein-poor and protein-rich regime from ~ 2 g L^{-1} at 10 mM to ~ 2.5 g L^{-1} at 200 mM. The effect of ionic strength was expected since the maximum adsorbed amount (Γ_{max}) increases with ionic strength as a result of a decrease of the effective radius (R_{eff}) (equation 6). This is confirmed by the fact that the curves superimpose when the data is corrected by $\Gamma_{mono,\ theory}$ according to equation 4 (figure 5C). As observed for the different proteins, F_s equals 2.

3.3. Application of the surface coverage model

As described above, for different proteins and at different ionic strength, the graph of $d_{3,2}$ as a function of $C(1- \Phi_{oil})Q_H/6\Phi_{oil}\Gamma_{mono,\ theory}$ shows a point where the emulsions reach the stable regime ($d_{3,2} = d_{3,2,\ min}$) (i.e. $C_{cr} = 2$). This point is named the stability factor (F_s) and has a value of 2 for all experiments. This shows that equation 3 can be applied to predict the droplet size for the obtained experimental data, when the stability factor of 2 is included (equation 12).

$$d_{3,2} = \frac{F_s 6\Phi_{oil}\Gamma_{mono,theory}}{(1-\Phi_{oil})Q_H C} \qquad (12)$$

In the current state, equation 12 is only a first order approximation describing the stability of emulsions as affected by ionic strength and concentration. Consequently, it needs further development (e.g. rationalization of the approach and validation for different conditions such as pH and Φ_{oil}). Still, the proposed model can be applied to other proteins, concentrates and isolates at different conditions (e.g. ionic strength, Φ_{oil}). Therefore, experimental data ($d_{3,2}$ as function of concentration) was collected from literature [5, 20, 23, 56]. Subsequently, the curves of the droplet size under these conditions were predicted using equations 2 and 12 assuming that Γ_{max} equals $\Gamma_{mono,\ theory}$ (equation 4) [14]. In addition, a Q_H of 0.73 for patatin [20] and 1.00 for whey protein isolate and concentrate (i.e. equal to β-lactoglobulin) were used (figure 6). The theoretical predictions of $d_{3,2}$ were in good agreement with the experimental results. This shows that even in the current form, the model already shows a quite good quantitative approximation of real, experimental data.

3.4. Predicting emulsion stability

Using the current model (i.e. so far approximating k_{adsorb} by Q_H), the critical protein concentration (C_{cr}) that separates the protein-poor from the protein-rich regime can be calculated for any protein under any condition using equation 13.

$$C_{cr} = \frac{F_s 6\Phi_{oil}\Gamma_{mono,theory}}{(1-\Phi_{oil})Q_H d_{3,2,\min}} \qquad (13)$$

The current model, as described in equation 13, only considers coalescence and flocculation as possible destabilization mechanism. In practice, creaming also plays an important role. The creaming rate of emulsion droplets (υ [m s^{-2}]) can be approximated by Stokes' law (equation 14).

$$\upsilon = \frac{2(\rho_d - \rho_c)gR^2}{9\eta_c} \qquad (14)$$

where ρ_d and ρ_c are the mass density of dispersed and continuous phase, respectively [kg m^{-3}], g is gravitational acceleration [9.80665 m s^{-2}], R is the radius of the emulsion droplet [m] and η_c is the viscosity of the continuous phase [kg s^{-1} m^{-1}].

If the creaming rate is in the order of 1 mm per day, creaming is considered negligible [57]. Therefore, the stability of an emulsion against destabilization can be predicted by combing equations 13 and 14 with a creaming rate of 1 mm/day (equation 15).

$$C_{cr} = \frac{F_s 6\Phi_{oil}\Gamma_{mono,theory}}{(1-\Phi_{oil})Q_H 2\sqrt{\frac{1.16\cdot10^{-8}\cdot 9\eta_c}{2(\rho_d - \rho_c)g}}} \qquad (15)$$

4. CONCLUSIONS

The stability of emulsions during formation is found to be affected by the same factors as the stability against flocculation after changes in conditions. In both cases, the stability is determined

by the coverage of the interface. A completely covered interface increases the stability against coalescence and flocculation. In addition to parameters related to the adsorbed layer (i.e. maximum adsorbed amount and interfacial area), the adsorption kinetics also affected the stability of the emulsion. Based on this information, the surface coverage model is proposed. The proposed model describes experimental data (i.e. droplet size) quantitatively and can therefore be used as a guideline to develop a more extended model for predicting the behaviour of protein-stabilized emulsions under different system conditions (i.e. pH and Φ_{oil}).

AUTHOR INFORMATION

Corresponding Author

*Phone: +31 317 483786

E-mail: peter.wierenga@wur.nl

Notes

The authors declare no competing financial interest.

REFERENCES

[1] Dickinson E. Adsorbed protein layers at fluid interfaces: interactions, structure and surface rheology. Colloids Surf, B. 1999;15:161-76.

[2] McClements DJ. Protein-stabilized emulsions. Curr Opin Colloid Interface Sci. 2004;9:305-13.

[3] Damodaran S. Protein stabilization of emulsions and foams. J Food Sci. 2005;70:R54-R66.

[4] Dickinson E. Flocculation of protein-stabilized oil-in-water emulsions. Colloids Surf, B. 2010;81:130-40.

[5] Tcholakova S, Denkov ND, Ivanov IB, Campbell B. Coalescence stability of emulsions containing globular milk proteins. Adv Colloid Interface Sci. 2006;123-126:259-93.

[6] Kim HJ, Decker EA, McClements DJ. Impact of protein surface denaturation on droplet flocculation in hexadecane oil-in-water emulsions stabilized by β-lactoglobulin. J Agric Food Chem. 2002;50:7131-7.

[7] Walstra P. Physical chemistry of foods. New York, NY, USA: Marcel Dekker, Inc.; 2003.

[8] Coupland JN, Weiss J, Lovy A, McClements DJ. Solubilization kinetics of triacyl glycerol and hydrocarbon emulsion droplets in a micellar solution. J Food Sci. 1996;61:1114-7.

[9] Li Y, Le Maux S, Xiao H, McClements DJ. Emulsion-based delivery systems for tributyrin, a potential colon cancer preventative agent. J Agric Food Chem. 2009;57:9243-9.

[10] Wooster TJ, Golding M, Sanguansri P. Impact of oil type on nanoemulsion formation and ostwald ripening stability. Langmuir. 2008;24:12758-65.

[11] Tcholakova S, Denkov ND, Sidzhakova D, Ivanov IB, Campbell B. Interrelation between drop size and protein adsorption at various emulsification conditions. Langmuir. 2003;19:5640-9.
[12] Tcholakova S, Denkov ND, Ivanov IB, Campbell B. Coalescence in β-lactoglobulin-stabilized emulsions: effects of protein adsorption and drop size. Langmuir. 2002;18:8960-71.
[13] Gurkov TD, Russev SC, Danov KD, Ivanov IB, Campbell B. Monolayers of globular proteins on the air/water interface: applicability of the Volmer equation of state. Langmuir. 2003;19:7362-9.
[14] Delahaije RJBM, Gruppen H, Giuseppin MLF, Wierenga PA. Quantitative description of the parameters affecting the adsorption behaviour of globular proteins. Colloids Surf, B. 2014;123:199-206.
[15] Adamczyk Z, Weroński P. Application of the DLVO theory for particle deposition problems. Adv Colloid Interface Sci. 1999;83:137-226.
[16] Johnson CA, Lenhoff AM. Adsorption of charged latex particles on mica studied by atomic force microscopy. J Colloid Interface Sci. 1996;179:587-99.
[17] Adamczyk Z, Szyk L. Kinetics of irreversible adsorption of latex particles under diffusion-controlled transport. Langmuir. 2000;16:5730-7.
[18] Delahaije RJBM, Wierenga PA, Giuseppin MLF, Gruppen H. Improved emulsion stability by succinylation of patatin is caused by partial unfolding rather than charge effects. J Colloid Interface Sci. 2014;430:69-77.
[19] Wierenga PA, Meinders MBJ, Egmond MR, Voragen AGJ, de Jongh HHJ. Protein exposed hydrophobicity reduces the kinetic barrier for adsorption of ovalbumin to the air-water interface. Langmuir. 2003;19:8964-70.
[20] Delahaije RJBM, Wierenga PA, van Nieuwenhuijzen NH, Giuseppin MLF, Gruppen H. Protein concentration and protein-exposed hydrophobicity as dominant parameters determining flocculation of protein-stabilized oil-in-water emulsions. Langmuir. 2013;29:11567-74.
[21] Qian C, McClements DJ. Formation of nanoemulsions stabilized by model food-grade emulsifiers using high-pressure homogenization: factors affecting particle size. Food Hydrocolloids. 2011;25:1000-8.
[22] Bouyer E, Mekhloufi G, Le Potier I, Du Fou de Kerdaniel T, Grossiord J-L, Rosilio V, et al. Stabilization mechanism of oil-in-water emulsions by β-lactoglobulin and gum arabic. J Colloid Interface Sci. 2011;354:467-77.
[23] Schwenzfeier A, Helbig A, Wierenga PA, Gruppen H. Emulsion properties of algae soluble protein isolate from *Tetraselmis sp.* Food Hydrocolloids. 2013;30:258-63.
[24] Bouyer E, Mekhloufi G, Huang N, Rosilio V, Agnely F. β-Lactoglobulin, gum arabic, and xanthan gum for emulsifying sweet almond oil: formulation and stabilization mechanisms of pharmaceutical emulsions. Colloids Surf, A. 2013;433:77-87.
[25] Kulmyrzaev AA, Schubert H. Influence of KCl on the physicochemical properties of whey protein stabilized emulsions. Food Hydrocolloids. 2004;18:13-9.
[26] Wierenga PA, Meinders MBJ, Egmond MR, Voragen AGJ, De Jongh HHJ. Quantitative description of the relation between protein net charge and protein adsorption to air-water interfaces. J Phys Chem B. 2005;109:16946-52.
[27] Feder J, Giaever I. Adsorption of ferritin. J Colloid Interface Sci. 1980;78:144-54.
[28] Dąbkowska M, Adamczyk Z. Mechanism of immonoglobulin G adsorption on mica-AFM and electrokinetic studies. Colloids Surf, B. 2014;118:57-64.
[29] Dąbkowska M, Adamczyk Z, Kujda M. Mechanism of HSA adsorption on mica determined by streaming potential, AFM and XPS measurements. Colloids Surf, B. 2013;101:442-9.
[30] Semmler M, Rička J, Borkovec M. Diffusional deposition of colloidal particles: electrostatic interaction and size polydispersity effects. Colloids Surf, A. 2000;165:79-93.
[31] Maranzano BJ, Wagner NJ. The effects of interparticle interactions and particle size on reversible shear thickening: hard-sphere colloidal dispersions. J Rheo. 2001;45:1205-22.
[32] Yuan Y, Oberholzer MR, Lenhoff AM. Size does matter: electrostatically determined surface coverage trends in protein and colloid adsorption. Colloids and Surfaces A: Physicochemical and Engineering Aspects. 2000;165:125-41.
[33] Kleimann J, Lecoultre G, Papastavrou G, Jeanneret S, Galletto P, Koper GJM, et al. Deposition of nanosized latex particles onto silica and cellulose surfaces studied by optical reflectometry. J Colloid Interface Sci. 2006;303:460-71.
[34] Brenner SL. A semiempirical model for the phase transition in polystyrene latexes. J Phys Chem. 1976;80:1473-7.
[35] Minton AP, Edelhoch H. Light scattering of bovine serum albumin solutions: extension of the hard particle model to allow for electrostatic repulsion. Biopolymers. 1982;21:451-8.
[36] Piech M, Walz JY. Analytical expressions for calculating the depletion interaction produced by charged spheres and spheroids. Langmuir. 2000;16:7895-9.

[37] Talbot J, Tarjus G, Van Tassel PR, Viot P. From car parking to protein adsorption: an overview of sequential adsorption processes. Colloids Surf, A. 2000;165:287-324.
[38] Feder J. Random sequential adsorption. J Theor Biol. 1980;87:237-54.
[39] Tanemura M. On random complete packing by discs. Ann Inst Stat Math. 1979;31:351-65.
[40] Finegold L, Donnell JT. Maximum density of random placing of membrane particles. Nature. 1979;278:443-5.
[41] Erickson HP. Size and shape of protein molecules at the nanometer level determined by sedimentation, gel filtration, and electron microscopy. Biol Proced Online. 2009;11:32-51.
[42] Israelachvili JN. Intermolecular and surface forces. Third ed. New York, NY, USA: Academic Press; 2011.
[43] Adamczyk Z, Weroński P. Random sequential adsorption of spheroidal particles: kinetics and jamming limit. J Chem Phys. 1996;105:5562-73.
[44] Elofsson UM, Paulsson MA, Arnebrant T. Adsorption of β-lactoglobulin A and B in relation to self-association: effect of concentration and pH. Langmuir. 1997;13:1695-700.
[45] Zhai J, Day L, Aguilar M-I, Wooster TJ. Protein folding at emulsion oil/water interfaces. Curr Opin Colloid Interface Sci. 2013;18:257-71.
[46] Rabe M, Verdes D, Seeger S. Understanding protein adsorption phenomena at solid surfaces. Adv Colloid Interface Sci. 2011;162:87-106.
[47] Seigel RR, Harder P, Dahint R, Grunze M, Josse F, Mrksich M, et al. On-line detection of nonspecific protein adsorption at artificial surfaces. Anal Chem. 1997;69:3321-8.
[48] Ramsden JJ. Concentration scaling of protein deposition kinetics. Phys Rev Lett. 1993;71:295-8.
[49] Wierenga PA, Egmond MR, Voragen AGJ, de Jongh HHJ. The adsorption and unfolding kinetics determines the folding state of proteins at the air-water interface and thereby the equation of state. J Colloid Interface Sci. 2006;299:850-7.
[50] Alizadeh-Pasdar N, Li-Chan ECY. Comparison of protein surface hydrophobicity measured at various pH values using three different fluorescent probes. J Agric Food Chem. 2000;48:328-34.
[51] Jachimska B, Wasilewska M, Adamczyk Z. Characterization of globular protein solutions by dynamic light scattering, electrophoretic mobility, and viscosity measurements. Langmuir. 2008;24:6866-72.
[52] Ruis HGM, van Gruijthuijsen K, Venema P, van der Linden E. Transitions in structure in oil-in-water emulsions as studied by diffusing wave spectroscopy. Langmuir. 2007;23:1007-13.
[53] Blijdenstein TBJ, Hendriks WPG, van der Linden E, van Vliet T, van Aken GA. Control of strength and stability of emulsion gels by a combination of long- and short-range interactions. Langmuir. 2003;19:6657-63.
[54] Höhler R, Cohen-Addad S, Durian DJ. Multiple light scattering as a probe of foams and emulsions. Curr Opin Colloid Interface Sci. 2014;19:242-52.
[55] Scheffold F. Particle sizing with diffusing wave spectroscopy. J Dispersion Sci Technol. 2002;23:591-9.
[56] van Koningsveld GA, Walstra P, Voragen AGJ, Kuijpers IJ, van Boekel MAJS, Gruppen H. Effects of protein composition and enzymatic activity on formation and properties of potato protein stabilized emulsions. J Agric Food Chem. 2006;54:6419-27.
[57] Kruyt HR. Colloid science. Amsterdam: Elsevier; 1952.

TABLES

Table 1. Protein properties obtained from literature.

Protein	**M_w[a] [kDa]**	**Q_H[b] [-]**	**$\Gamma_{mono,theory}$[b] [mg m^{-2}]**	**ζ Potential[b] [mV]**
β-Lactoglobulin	18.3	0.52	1.62[c]	-21.2
Ovalbumin	42.8	0.10	1.73	-16.5
Lysozyme	14.3	0.03	1.58	2.0

[a]values obtained from the Swiss-Prot database (http://www.expasy.org). [b]literature values[14]. [c]$\Gamma_{mono,\ theory}$ for a β-lactoglobulin dimer.

FIGURE CAPTIONS

Figure 1. Effect of low and high protein concentration on the emulsion stability against coalescence during formation (A) and against flocculation after formation (B). The dark and light grey circles represent the protein and the Debye screening length, respectively. The effective radius of an adsorbed protein is a combination of protein and the Debye screening length.

Figure 2. Average droplet size ($d_{3,2}$) as function of protein concentration (A) and as function of $C(1-\Phi_{oil})/6\Phi_{oil}\Gamma_{max}$ (B) calculated from equation 1 with a $d_{3,2,\ min}$ of 1 μm (equation 2) for emulsions with Φ_{oil} = 0.2 and Γ_{max} = 3 mg m^{-2} (1), Φ_{oil} = 0.2 and Γ_{max} = 5 mg m^{-2} (2) and Φ_{oil} = 0.4 and Γ_{max} = 3 mg m^{-2} (3). The grey area in figure B represents the protein-poor regime.

Figure 3. Decay time ($\tau_{1/2}$) as a function of the absolute zeta potential for emulsion droplets stabilized by β-lactoglobulin at 2 g L^{-1} (◇), 5 g L^{-1} (□), and 2 g L^{-1} supplemented to a concentration of 5 g L^{-1} (○) (pH = 7.0 and Φ_{oil} = 0.1). The solid lines are guides to the eye.

Figure 4. Decay time ($\tau_{1/2}$) (A) and average droplet size ($d_{3,2}$) (B) as function of protein concentration and average droplet size as function of $C(1-\Phi_{oil})/6\Phi_{oil}\Gamma_{max}$ (C) and as function of $C(1-\Phi_{oil})Q_H/6\Phi_{oil}\Gamma_{max}$ (D) for emulsions stabilized by β-lactoglobulin (◇), ovalbumin (△) and lysozyme (□) (pH = 7.0, I = 10 mM and Φ_{oil} = 0.1). The grey area in figure D represents the protein-poor regime. The inserts show the small droplet size regime. Lines are guides to the eye.

Figure 5. Concentration dependence of the decay time ($\tau_{1/2}$) (A), average droplet size ($d_{3,2}$) (B) and average droplet size as function of $C(1-\Phi_{oil})Q_H/6\Phi_{oil}\Gamma_{mono,theory}$ (C) for

569 β-lactoglobulin-stabilized emulsions at an ionic strength of 10 mM (◇) and 200 mM (△) (pH =
570 7.0 and Φ_{oil} = 0.1). The grey areas in A and B represent the protein-poor regime at ionic strength
571 of 10 (light grey) and 200 mM (dark grey). The grey area in C represents the protein-poor
572 regime. The inserts show the small droplet size regime.
573
574 **Figure 6.** Average droplet size ($d_{3,2}$) for emulsions stabilized by β-lactoglobulin (pH = 7.0, I =
575 10 mM and Φ_{oil} = 0.1)[20] (A), patatin (pH = 7.0, I = 50 mM and Φ_{oil} = 0.1)[56] (B), whey
576 protein isolate (pH = 7.0, I = 10 mM and Φ_{oil} = 0.3)[23] (C) and whey protein concentrate (pH =
577 7.0, I = 150 mM and Φ_{oil} = 0.28)[21] (D). The dashed lines represent the fit of the data using
578 equations 2 and 3, with $k_{adsorb} = Q_H$.
579

580 FIGURES

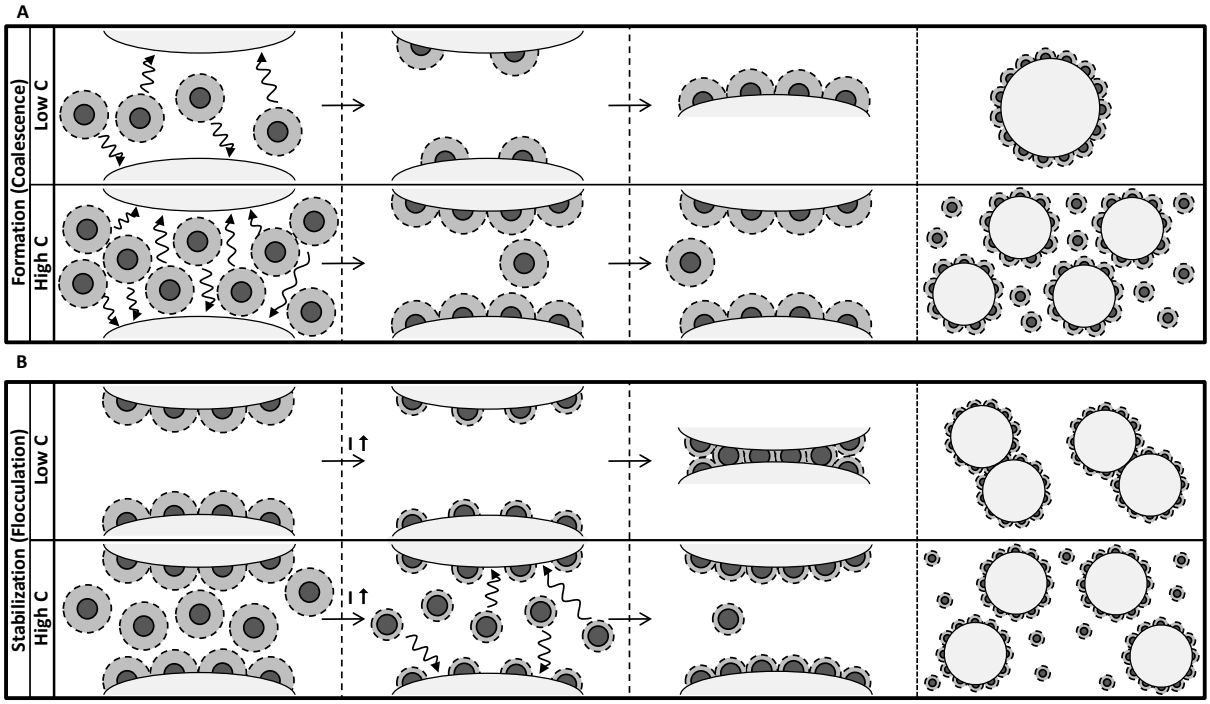

581

582

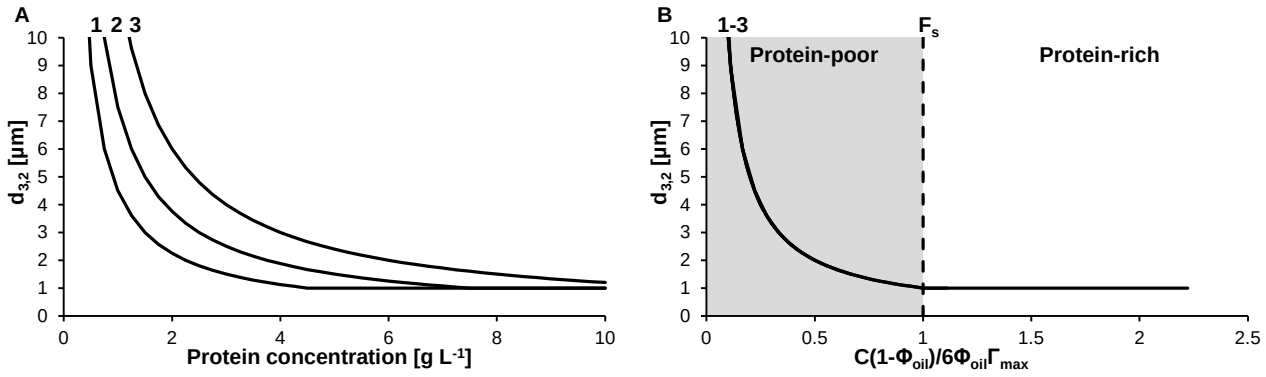
A
1 2 3
$d_{3,2}$ [µm]
Protein concentration [g L^{-1}]
B
1-3
F_s
Protein-poor
Protein-rich
$d_{3,2}$ [µm]
$C(1-\Phi_{oil})/6\Phi_{oil}\Gamma_{max}$

583

584

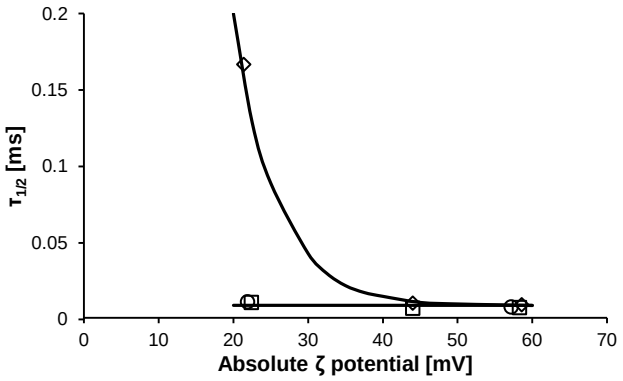
0.2
0.15
0.1
0.05
0
$\tau_{1/2}$ [ms]
0
10
20
30
40
50
60
70
Absolute ζ potential [mV]

585

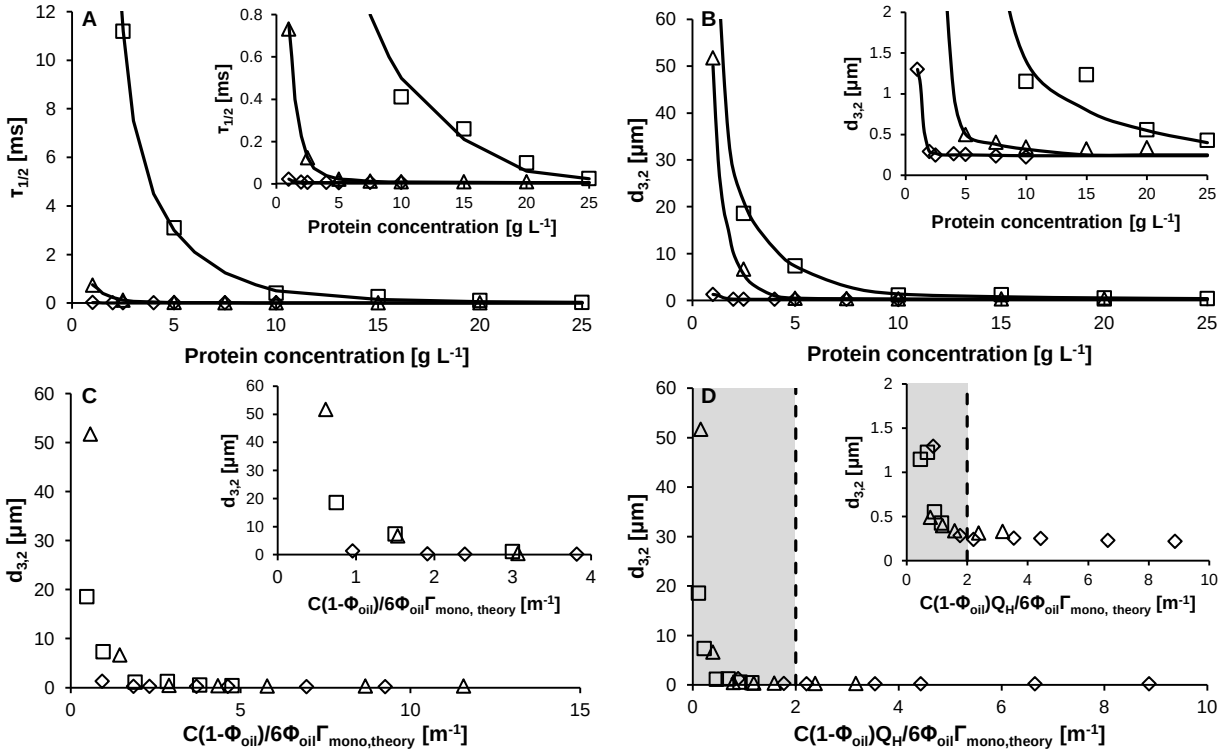
A
$\tau_{1/2}$ [ms]
Protein concentration [g L^{-1}]
B
$d_{3,2}$ [µm]
Protein concentration [g L^{-1}]
C
$d_{3,2}$ [µm]
C(1-Φ_{oil})/6$\Phi_{oil}\Gamma_{mono,theory}$ [m^{-1}]
D
$d_{3,2}$ [µm]
C(1-Φ_{oil})Q_H/6$\Phi_{oil}\Gamma_{mono,theory}$ [m^{-1}]

586

587

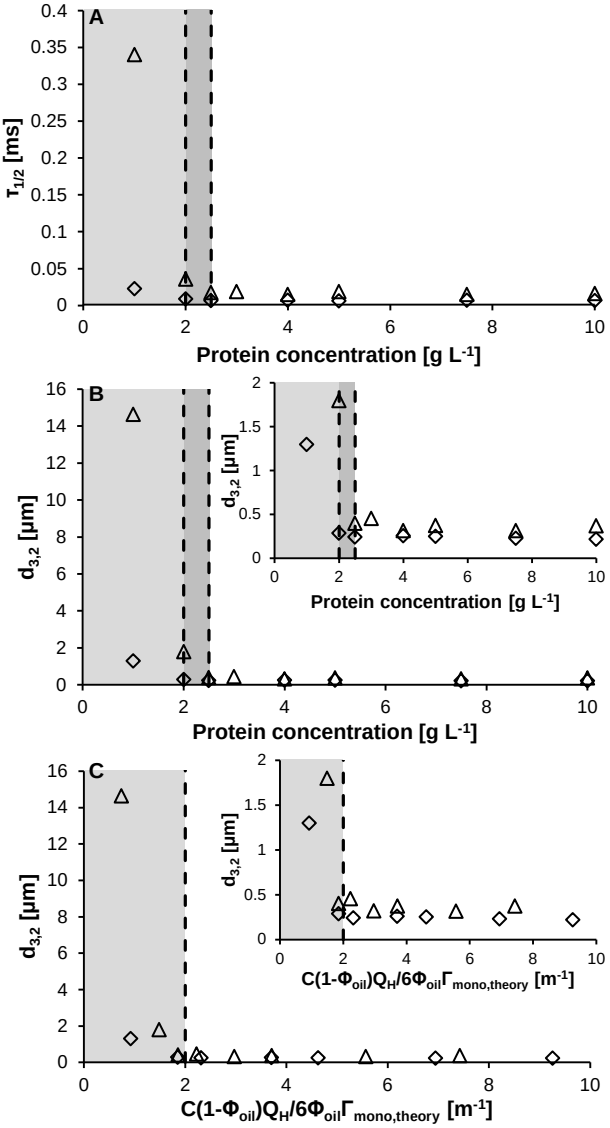
A
$\tau_{1/2}$ [ms]
Protein concentration [g L^{-1}]
B
$d_{3,2}$ [µm]
Protein concentration [g L^{-1}]
C
$d_{3,2}$ [µm]
$C(1-\Phi_{oil})Q_H/6\Phi_{oil}\Gamma_{mono,theory}$ [m^{-1}]

588

589

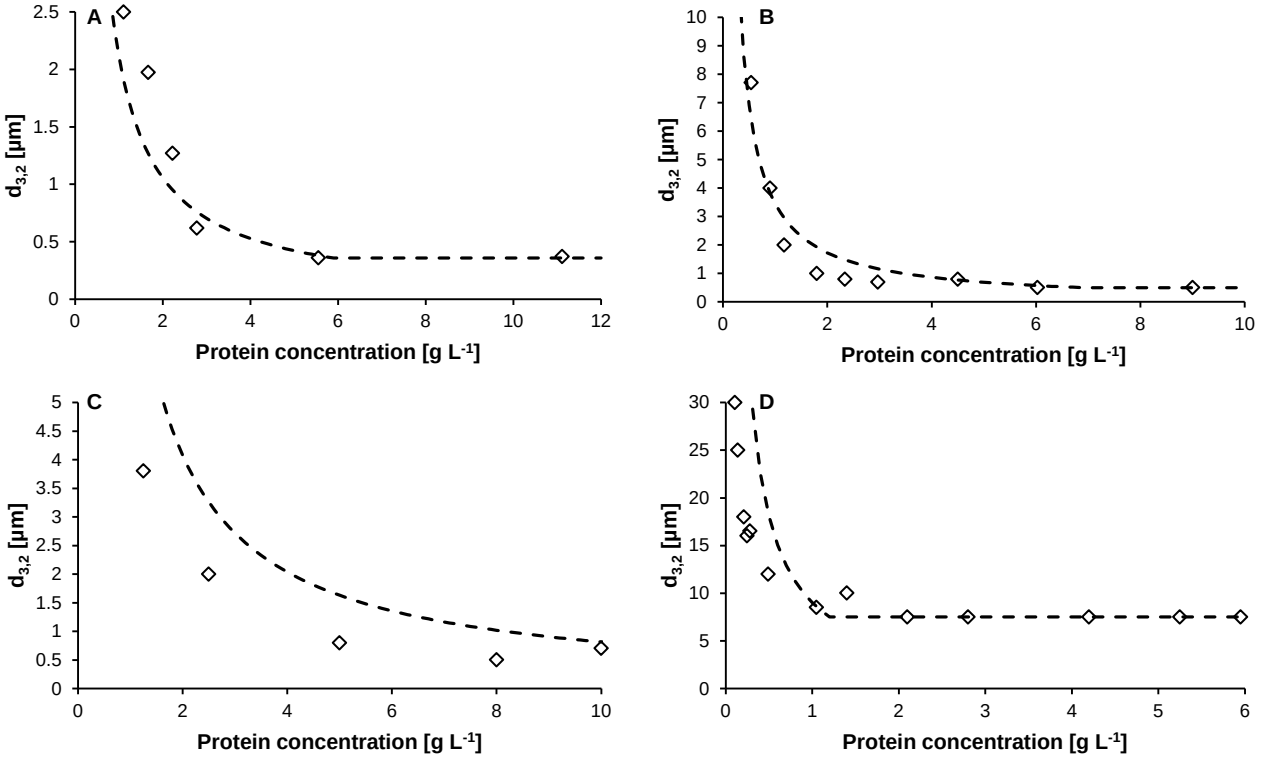

590

591

592